

ADJOINT METHODS IN CFD-BASED OPTIMIZATION - GRADIENT COMPUTATION & BEYOND

**Kyriakos C. Giannakoglou¹, Dimitrios I. Papadimitriou¹,
Evangelos M. Papoutsis-Kiachagias¹ and Carsten Othmer²**

¹National Technical University of Athens,
School of Mechanical Engineering,
Lab. Of Thermal Turbomachines,
Parallel CFD & Optimization Unit
Zografou, Athens, 15710, Greece
e-mails: kgianna@central.ntua.gr, dpapadim@mail.ntua.gr, vaggelisp@gmail.com

²Volkswagen AG, CAE Methods, Group Research,
Letter Box 1777, D-38436 Wolfsburg, Germany
e-mail: carsten.othmer@volkswagen.de

Keywords: adjoint approach, Hessian matrix, shape and topology optimization, optimal active flow control, robust design

Abstract. *An overview of recent achievements in the development of adjoint-based methods and tools in the fields of aero/hydrodynamic shape optimization, optimal active flow control and topology optimization, in compressible and incompressible flows, is presented. In the first part, the continuous adjoint approach to widely-used turbulence models, such as the low-Reynolds Spalart-Allmaras and the high-Reynolds $k-\varepsilon$ ones is discussed. The relevant developments allow the computation of the exact gradient of the objective function using continuous adjoint, even for RANS assisted by wall functions, and overcome the frequently made assumption of negligible turbulence variations. The second part of this paper deals with higher-order sensitivity analysis based on the combined use of the adjoint approach and direct differentiation. Through the methods exposed herein, the aforementioned optimization problems can be solved faster via the Newton's method; also, robust design problems can be tackled using gradient-based algorithms. For large scale problems, the fact that the computational cost scales with the number of design variables is overcome using truncated Newton or the exactly initialized quasi-Newton method. For robust design problems, the computation of second-order derivatives w.r.t. the environmental variables is necessary; if in addition, the problem is to be solved using a descent algorithm, third-order mixed derivatives w.r.t. both environmental and design variables must be available; optimal ways to perform these computations are demonstrated. This paper goes through both continuous and (hand-differentiated) discrete adjoint methods; some topics are, however, presented by emphasizing on the continuous approach, where the relevant literature is quite poor.*

1 INTRODUCTION

This paper presents the continuous and discrete adjoint method for the computation and use of the first- and higher-order sensitivity derivatives of objective functions F in optimization problems governed by PDEs, in aero/hydrodynamics. The paper starts by the development of the continuous adjoint method to low-Reynolds turbulence models by focusing on the need to include the adjoint turbulence model equations into the optimization loop; such a treatment maximizes accuracy and avoids the computation of wrongly-signed derivatives which may mislead the search algorithm. Apart from low-Reynolds turbulent models, the continuous adjoint method to high-Reynolds turbulence models, relying on the wall function technique, is presented. Despite their reduced accuracy in complex flows, wall function based models are still in use in industrial applications, allowing computations on coarser grids with lower computational cost. The adjoint wall function technique allows the computation of the exact gradient, based on wall functions. The adjoint method for the computation of (exact) second-order derivatives or the Hessian matrix of F is, then, presented. The availability of such a method allows the use of the (exact) Newton method, instead of either quasi-Newton methods (such as BFGS, etc.) or the much simpler but less efficient steepest descent. Whether Newton's method is more efficient than its aforementioned counterparts or not depends on the cost for computing the Hessian. The exactly-initialized quasi-Newton and the truncated Newton methods, being more efficient alternatives to the exact Newton method are also presented. The truncated Newton is an elegant way to avoid the costly computation of the Hessian matrix, since products of the Hessian matrix with vectors are only needed; it is shown that this noticeably decreases the CPU cost, without damaging accuracy. The similarity of ways to compute the Hessian based on either discrete or continuous approaches is discussed. The adjoint method for the solution of robust design problems is presented. It is based on the second-order second-moment (SOSM) approach and a gradient-based algorithm, requiring up to third-order mixed derivatives (w.r.t. the environmental and design variables) to be available.

Regarding applications, the adjoint method is demonstrated for various objective functions and used to solve aero/hydrodynamic shape optimization problems, optimization of jet-based flow-control systems for controlling the development of boundary layers and topology optimization problems in fluid mechanics. Depending on the problem, the development relies upon the incompressible or compressible fluid flow equations.

The adjoint solvers used herein have been programmed on a time-marching, primitive-variable, in-house flow solver, for both incompressible and compressible flows (finite-volume discretization, vertex-centered storage; pseudo-compressibility method for incompressible flows; fully parallelized and GPU-enabled code [1], [2]) and the OpenFOAM software, for incompressible flows. The turbulence models which are used are the low-Reynolds number Spalart-Allmaras one-equation model and the high-Reynolds number $k-\epsilon$ model, with wall functions.

Recall that, in the continuous adjoint approach, [3, 4, 5, 6, 7, 8, 9, 10, 11], the adjoint PDEs and their boundary conditions are derived from the flow (or primal or state) PDEs and their boundary conditions and, then, discretized and numerically solved. In contrast, the discrete adjoint approach, [12, 13, 14, 15], relies on adjoint equations which result, directly in discrete form, from the discretized state equations.

2 AERODYNAMIC OPTIMIZATION IN TURBULENT FLOWS

2.1 Flow Equations and Objective Functions

To avoid duplicating the presented material throughout this paper, the development is based on the most general case of turbulent flows with heat transfer. In this section, incompressible fluid flows are considered. The system of primal equations is valid for shape, topology or flow control optimization problems; to also include topology optimization, additional terms depending on the so-called porosity variable α are appended to the conventional equations. The extra terms must be zeroed ($\alpha \equiv 0$) in shape or flow control optimization; they play, however, a critical role in topology optimization (see section 2.4). As in [3], the Spalart-Allmaras turbulence model is used. Based on the above, the state equations are symbolically written as

$$R^p = 0, \quad R^{v_i} = 0, \quad R^T = 0, \quad R^{\tilde{\nu}} = 0 \quad (1)$$

where

$$R^p = \frac{\partial v_j}{\partial x_j} \quad (2)$$

$$R^{v_i} = v_j \frac{\partial v_i}{\partial x_j} + \frac{\partial p}{\partial x_i} - \frac{\partial}{\partial x_j} \left[(\nu + \nu_t) \left(\frac{\partial v_i}{\partial x_j} + \frac{\partial v_j}{\partial x_i} \right) \right] + \alpha v_i \quad (3)$$

$$R^T = v_j \frac{\partial T}{\partial x_j} - \frac{\partial}{\partial x_j} \left[\left(\frac{\nu}{Pr} + \frac{\nu_t}{Pr_t} \right) \frac{\partial T}{\partial x_j} \right] + \alpha (T - T_{wall}) \quad (4)$$

$$R^{\tilde{\nu}} = v_j \frac{\partial \tilde{\nu}}{\partial x_j} - \frac{\partial}{\partial x_j} \left[\left(\nu + \frac{\tilde{\nu}}{\sigma} \right) \frac{\partial \tilde{\nu}}{\partial x_j} \right] - \frac{c_{b2}}{\sigma} \left(\frac{\partial \tilde{\nu}}{\partial x_j} \right)^2 - \tilde{\nu} P(\tilde{\nu}) + \tilde{\nu} D(\tilde{\nu}) + \alpha \tilde{\nu} \quad (5)$$

Here, v_i are the velocity components, p is the static pressure divided by the density, T is the static temperature, $\tilde{\nu}$ is the turbulence state variable, ν is the bulk viscosity and ν_t is the turbulent viscosity given by

$$\nu_t = \tilde{\nu} f_{v_t} \quad (6)$$

Also, Pr , Pr_t are the laminar and turbulent Prandtl numbers and T_{wall} is the known temperature along the walls surrounding the flow which is used only in a particular class of topology optimization problems. Depending on the application in hand, $R^{\tilde{\nu}}$ must be ignored in laminar flows and so does R^T if heat transfer effects are of no interest. The applications presented in this paper are dealing the following objective functions: (1) the volume-averaged total pressure losses between the inlet S_I and the outlet S_O of the domain Ω , (2) the force exerted on the solid walls S_W along a user-defined direction r_i , (3) the volume-averaged temperature difference between S_O and S_I , (4) the generation of entropy E in the flow passage, (5) the deviation of the hydraulic head H from a desirable value H_{tar} (for hydraulic turbomachines) and (6) the deviation of the pressure distribution p from a given distribution p_{tar} along S_w (inverse design

problems). The aforementioned functions, to be minimized, are defined below

$$F_1 = \int_{S_I} F_{S_I} dS + \int_{S_O} F_{S_O} dS = - \int_{S_I} \left(p + \frac{1}{2} v^2 \right) v_i n_i dS - \int_{S_O} \left(p + \frac{1}{2} v^2 \right) v_i n_i dS \quad (7)$$

$$F_2 = \int_{S_W} F_{S_W} dS = \int_{S_W} \left[-(\nu + \nu_t) \left(\frac{\partial v_i}{\partial x_j} + \frac{\partial v_j}{\partial x_i} \right) + p \delta_i^j \right] n_j r_i dS \quad (8)$$

$$F_3 = - \int_{S_I} T v_i n_i dS - \int_{S_O} T v_i n_i dS \quad (9)$$

$$F_4 = \int_{\Omega} \rho v_i \frac{\partial E}{\partial x_i} d\Omega \quad (10)$$

$$F_5 = \frac{1}{2} (H - H_{tar})^2 \quad (11)$$

$$F_6 = \frac{1}{2} \int_{S_w} (p - p_{tar})^2 dS \quad (12)$$

In hydraulic turbomachines, the head H is given by

$$H = \frac{\int_{S_I} \left(p + \frac{1}{2} v_k^2 \right) v_i n_i dS + \int_{S_O} \left(p + \frac{1}{2} v_k^2 \right) v_i n_i dS}{g \int_{S_I} v_i n_i dS} \quad (13)$$

where n_i is the outward unit normal vector and g the gravitational acceleration.

2.2 The Adjoint Method for Shape Optimization in Turbulent Flows

One of the most important issues regarding the development of adjoint methods, particularly those based on the continuous approach, is the handling of turbulence models. Though in discrete adjoint the differentiation of the already discretized turbulence model equations is straightforward and can be found in several published works, [16, 17, 18], in continuous adjoint the majority of the existing works rely on the so-called ‘‘frozen turbulence’’ assumption. Based on this assumption, sensitivities of the turbulence quantities w.r.t. the design variables are neglected. The first work presenting the adjoint to one of the most widely used turbulence models, namely the Spalart-Allmaras one, for incompressible flows, is [3]. Later on, this was extended to compressible flows in [19]. Regarding the adjoint approach to high-Reynolds turbulence models, the (continuous) adjoint to the k - ε model with wall functions was just recently presented in the literature, [4].

This section aims at briefly presenting the underlying adjoint developments and convincing the reader that, in some cases, the development and solution of the adjoint turbulence model equation(s) is really necessary.

The continuous adjoint approach for handling shape optimization problems (with $\alpha \equiv 0$) is presented in this subsection. A brief discussion of the equivalent discrete approach can be found in the beginning of subsection 3.1. The total sensitivity derivatives (symbol δ) of any function Φ w.r.t. the design variables b_m are related to its partial sensitivities (symbol ∂) through the relation

$$\frac{\delta \Phi}{\delta b_m} = \frac{\partial \Phi}{\partial b_m} + \frac{\partial \Phi}{\partial x_l} \frac{\delta x_l}{\delta b_m} \quad (14)$$

where $\frac{\delta x_l}{\delta b_m}$ are the sensitivities of nodal coordinates. The augmented objective function F_{aug} is defined as the sum of F and field integrals of the products of the adjoint variable fields and the

state equations, as follows

$$F_{aug} = \int_{\Omega} u_i R_i^v d\Omega + \int_{\Omega} q R^p d\Omega + \int_{\Omega} T_a R^T d\Omega + \int_{\Omega} \tilde{v}_a R^{\tilde{v}} d\Omega \quad (15)$$

where u_i are the adjoint velocity components, q is the adjoint pressure, T_a the adjoint temperature and \tilde{v}_a the adjoint to \tilde{v} . Based on the Leibniz theorem, the variation of F_{aug} w.r.t. b_m reads

$$\begin{aligned} \frac{\delta F_{aug}}{\delta b_m} &= \frac{\delta F}{\delta b_m} + \int_{\Omega} u_i \frac{\partial R_i^v}{\partial b_m} d\Omega + \int_{\Omega} q \frac{\partial R^p}{\partial b_m} d\Omega + \int_{\Omega} T_a \frac{\partial R^T}{\partial b_m} d\Omega + \int_{\Omega} \tilde{v}_a \frac{\partial R^{\tilde{v}}}{\partial b_m} d\Omega \\ &+ \int_S u_i R_i^v \frac{\delta x_k}{\delta b_m} n_k dS + \int_S q R^p \frac{\delta x_k}{\delta b_m} n_k dS + \int_S T_a R^T \frac{\delta x_k}{\delta b_m} n_k dS \\ &+ \int_S \tilde{v}_a R^{\tilde{v}} \frac{\delta x_k}{\delta b_m} n_k dS \end{aligned} \quad (16)$$

where $S = S_I \cup S_O \cup S_w$. Through the Gauss divergence theorem, eq. 16 becomes

$$\begin{aligned} \frac{\delta F_{aug}}{\delta b_m} &= \int_{\Omega} R_i^u \frac{\partial v_i}{\partial b_m} d\Omega + \int_{\Omega} R^q \frac{\partial p}{\partial b_m} d\Omega + \int_{\Omega} R^{T_a} \frac{\partial T}{\partial b_m} d\Omega + \int_{\Omega} R^{\tilde{v}_a} \frac{\partial \tilde{v}}{\partial b_m} d\Omega \\ &+ \int_S B_i^u \frac{\partial v_i}{\partial b_m} dS + \int_S B_{ij}^{G_u} \frac{\partial}{\partial b_m} \left(\frac{\partial v_i}{\partial x_j} \right) dS + \int_S B^q \frac{\partial p}{\partial b_m} dS + \int_S B^{T_a} \frac{\partial T}{\partial b_m} dS \\ &+ \int_S B_i^{GT} \frac{\partial}{\partial b_m} \left(\frac{\partial T}{\partial x_i} \right) dS + \int_S B^{\tilde{v}_a} \frac{\partial \tilde{v}}{\partial b_m} dS + \int_S B_i^{G_{\tilde{v}_a}} \frac{\partial}{\partial b_m} \left(\frac{\partial \tilde{v}}{\partial x_i} \right) dS + SD \end{aligned} \quad (17)$$

Some of the integrands (such as R_i^u , etc.) are defined below and the remaining ones (such as B_i^u , etc.) can be found in [3]. SD is a sum of integrals (see eq. 22) which depend only on the sensitivities of geometrical quantities and, thus, leads to the expression of sensitivity derivatives of F . The elimination of all field (Ω) integrals depending on the sensitivities of the flow variables ($\frac{\partial v_i}{\partial b_m}$, etc.) gives rise to the adjoint mean flow and turbulence equations, as follows

$$R^q = \frac{\partial u_j}{\partial x_j} = 0 \quad (18)$$

$$\begin{aligned} R^{u_i} &= -v_j \left(\frac{\partial u_i}{\partial x_j} + \frac{\partial u_j}{\partial x_i} \right) + \frac{\partial q}{\partial x_i} - \frac{\partial}{\partial x_j} \left[(\nu + \nu_t) \left(\frac{\partial u_i}{\partial x_j} + \frac{\partial u_j}{\partial x_i} \right) \right] \\ &- \tilde{v} \frac{\partial \tilde{v}_a}{\partial x_i} - \frac{\partial}{\partial x_k} \left(e_{jki} e_{jmq} \frac{C_S(\tilde{v})}{S} \frac{\partial v_q}{\partial x_m} \tilde{v} \tilde{v}_a \right) - T \frac{\partial T_a}{\partial x_i} + \alpha u_i = 0 \end{aligned} \quad (19)$$

$$R^{T_a} = -v_j \frac{\partial T_a}{\partial x_j} - \frac{\partial}{\partial x_j} \left[\left(\frac{\nu}{Pr} + \frac{\nu_t}{Pr_t} \right) \frac{\partial T_a}{\partial x_j} \right] + \alpha T_a = 0 \quad (20)$$

$$\begin{aligned} R^{\tilde{v}_a} &= -v_j \frac{\partial \tilde{v}_a}{\partial x_j} - \frac{\partial}{\partial x_j} \left[\left(\nu + \frac{\tilde{v}}{\sigma} \right) \frac{\partial \tilde{v}_a}{\partial x_j} \right] + \frac{1}{\sigma} \frac{\partial \tilde{v}_a}{\partial x_j} \frac{\partial \tilde{v}}{\partial x_j} + 2 \frac{c_{b2}}{\sigma} \frac{\partial}{\partial x_j} \left(\tilde{v}_a \frac{\partial \tilde{v}}{\partial x_j} \right) + (D - P) \tilde{v}_a \\ &+ \tilde{v}_a \tilde{v} C_{\tilde{v}}(\tilde{v}, \tilde{v}) + \frac{\delta \nu_t}{\delta \tilde{v}} \frac{\partial u_i}{\partial x_j} \left(\frac{\partial v_i}{\partial x_j} + \frac{\partial v_j}{\partial x_i} \right) + \frac{\delta \nu_t}{\delta \tilde{v}} \frac{1}{Pr_t} \frac{\partial T_a}{\partial x_j} \frac{\partial T}{\partial x_j} + \alpha \tilde{v}_a = 0 \end{aligned} \quad (21)$$

where $\alpha \equiv 0$. The elimination of the boundary integrals that depend on the sensitivities of the flow variables yields the adjoint boundary conditions, as exposed in detail in [3]. The remaining

integrals (terms abbreviated to SD in eq. 17) define the sensitivity derivatives of F w.r.t. the design variables b_m , namely

$$\begin{aligned} \frac{\delta F}{\delta b_m} = & \int_{S_W} \frac{\partial F_{S_W}}{\partial x_k} \frac{\delta x_k}{\delta b_m} dS + \int_{S_W} F_{S_W} \frac{\delta(dS)}{\delta b_m} - \int_{S_W} \left[\nu \left(\frac{\partial u_i}{\partial x_j} + \frac{\partial u_j}{\partial x_i} \right) n_j - q n_i \right] \frac{\partial v_i}{\partial x_k} \frac{\delta x_k}{\delta b_m} dS \\ & + \int_{S_W} u_i R_i^v \frac{\delta x_k}{\delta b_m} n_k dS + \int_{S_W} q R^p \frac{\delta x_k}{\delta b_m} n_k dS + \int_{S_W} \nu \frac{\partial F_{S_W}}{\partial p} \frac{\partial}{\partial x_k} \left(\frac{\partial v_i}{\partial x_j} + \frac{\partial v_j}{\partial x_i} \right) \frac{\delta x_k}{\delta b_m} n_i n_j dS \\ & + \int_{S_W} \nu \frac{\partial F_{S_W}}{\partial p} \left(\frac{\partial v_i}{\partial x_j} + \frac{\partial v_j}{\partial x_i} \right) \frac{\delta(n_i n_j)}{\delta b_m} dS - \int_{S_W} \nu \frac{\partial \tilde{v}_a}{\partial x_j} n_j \frac{\partial \tilde{v}}{\partial x_k} \frac{\delta x_k}{\delta b_m} dS + \int_{\Omega} \tilde{v}_a \tilde{v} \mathcal{C}_{\Delta}(\tilde{v}, \vec{v}) \frac{\partial \Delta}{\partial b_m} d\Omega \end{aligned} \quad (22)$$

where $\mathcal{C}_S(\tilde{v})$, $\mathcal{C}_{\tilde{v}}(\tilde{v}, \vec{v})$ and $\mathcal{C}_{\Delta}(\tilde{v}, \vec{v})$ result from the Spalart–Allmaras model equations. Terms such as $\frac{\delta x_k}{\delta b_m}$, $\frac{\delta(dS)}{\delta b_m}$, $\frac{\delta(n_i n_j)}{\delta b_m}$, etc. depend on the selected parameterization scheme for the shape (S_w) to be designed and can readily be computed either numerically or analytically. Note that $\frac{\delta F}{\delta b_m}$ are all expressed as integrals along S_W with the exception of the last integral in eq. 22 which is a field integral the sensitivities of nodal distances Δ from the solid walls.

Fig. 1 shows an indicative example which convincingly proves that the omission of solving the adjoint turbulence model equation(s) (i.e. in the analyzed example, the omission of solving eq. 21) may mislead the optimization by computing derivatives $\frac{\delta F}{\delta b_m}$ with the wrong sign.

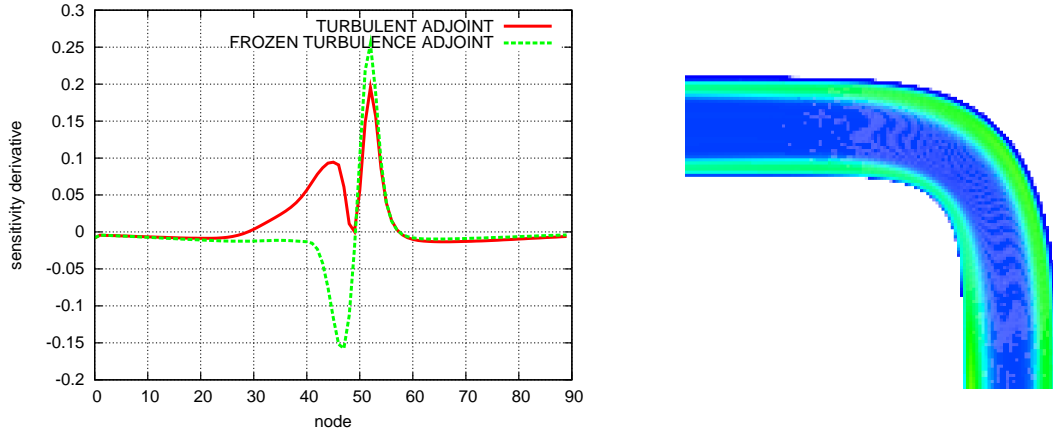


Figure 1: Shape optimization of an elbow duct for min. $F = F_1$, (eq. 7). Sensitivity derivatives $\frac{\delta F}{\delta b_m}$ (left), where b_m are the normal displacements of the solid wall grid nodes. Two sensitivity distributions were compared (a) by solving the complete adjoint system, including the adjoint to the turbulence model PDEs (marked as “turbulent adjoint”) and (b) by making the “frozen turbulence” assumption. The abscissa stands for the IDs of the inner wall nodes. It is clear that, by making the “frozen turbulence” assumption, wrongly signed sensitivities are computed for nodes 20 to 50. The velocity isolines are also plotted (right).

The previous development was based on the low-Reynolds number Spalart–Allmaras model. However, several engineering applications still rely on high-Reynolds number turbulence models with wall functions, since their use allows handling coarser grids and saving computational cost. For this reason, in [4], the continuous adjoint approach to the high-Reynolds $k-\varepsilon$ turbulence model, [20], was presented for incompressible flows. In the system of flow equations, the PDEs for k and ε replace eq. 5; eq. 6 is also replaced by $\nu_t = c_\mu \frac{k^2}{\varepsilon}$. In the interest of space, we refrain from presenting these equations in detail. Applying the wall function technique means that the k and ε values at the first nodes off the wall are all expressed in terms of the local friction velocity v_τ , where

$$v_\tau^2 = (\nu + \nu_t) \left(\frac{\partial v_i}{\partial x_j} + \frac{\partial v_j}{\partial x_i} \right) n_j t_i \quad (23)$$

Consequently, during the development of the adjoint formulation, an integral depending on $\frac{\delta v_\tau}{\delta b_m}$ (instead of the sensitivities of k , ε and v_i) appears along S_w . The elimination of this integral leads to the definition of a new quantity, to be referred to as the local adjoint friction velocity,

$$u_\tau^2 = (\nu + \nu_t) \left(\frac{\partial u_i}{\partial x_j} + \frac{\partial u_j}{\partial x_i} \right) n_j t_i \quad (24)$$

which, similarly to eq. 23, is expressed in terms of the local gradient of the adjoint velocities. Since differentiation close to the wall must be avoided, the squared adjoint friction velocity is computed by the expression, [4],

$$u_\tau^2 = \frac{1}{c_v} \left[2u_k t_k v_\tau - \left(\nu + \frac{\nu_t}{Pr_k} \right) \frac{\partial k_a}{\partial x_j} n_j \frac{\delta k}{\delta v_\tau} - \left(\nu + \frac{\nu_t}{Pr_\varepsilon} \right) \frac{\partial \varepsilon_a}{\partial x_j} n_j \frac{\delta \varepsilon}{\delta v_\tau} \right] \quad (25)$$

and serves to apply the wall boundary conditions for the adjoint momentum equations. An indicative application of the adjoint wall function technique is shown in fig. 2

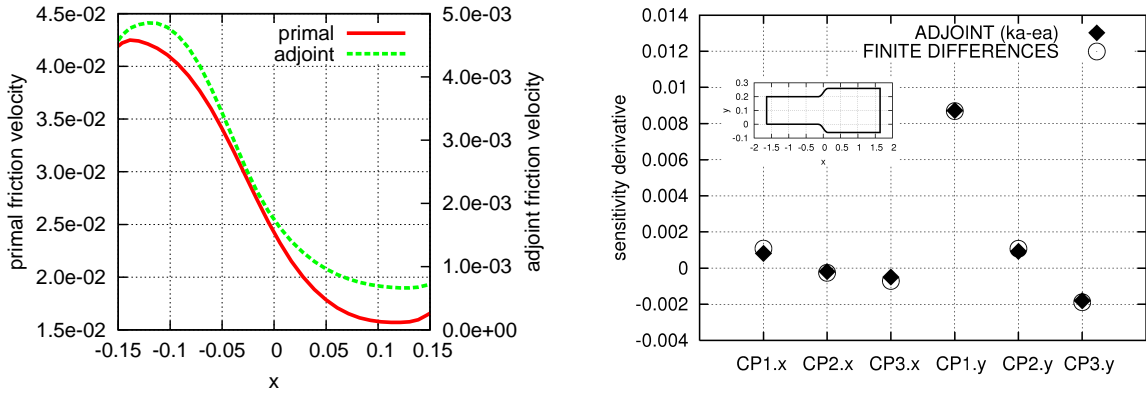


Figure 2: Optimization of an axial diffuser using the adjoint wall function technique, for min. $F = F_1$, (eq. 7). Left: Friction velocity v_τ and squared adjoint friction velocity u_τ^2 distributions along its lower wall. Right: Sensitivity derivatives of F w.r.t. the design variables, i.e. the coordinates of Bézier control points parameterizing its side walls. The adjoint wall function method perfectly matches the sensitivity derivatives computed using finite differences (FD).

2.3 The Adjoint Method for the Optimal Active Flow Control

This section presents a different use of the continuous adjoint method. Here, the adjoint method is used as a tool to identify the appropriate location and “type” (suction or blowing) of steady jets used in active flow control systems. Sensitivity maps are plotted along S_w and, based on them, the designer extracts information about the optimal location (from the sensitivity magnitude) and “type” (from the sensitivity sign) of the jet to be applied, so as to successfully control the boundary layer development. Jets are used to prevent or delay separation, control transition from laminar to turbulent flow, suppress or enhance turbulence, control shock waves and their interactions with boundary layers, etc. [21, 22].

In such a problem, the design variables are the values of the Cartesian components of hypothetical jet velocities v_{pq}^b ($p \in [1, 2]$ in 2D or $p \in [1, 3]$ in 3D problems) at the N wall boundary nodes ($q \in [1, N]$). Since $\frac{\delta x_k}{\delta b_i} = 0$, it can be proved that, at any point over S_w , the sensitivity derivatives are

$$\frac{1}{\Delta S_q} \frac{\delta F}{\delta v_{pq}^b} = v_{eff} \left(\frac{\partial u_{pq}}{\partial x_j} + \frac{\partial u_{jq}}{\partial x_p} \right) n_{jq} - q_q n_{pq} \quad (26)$$

Note that, for eq. 26 to be valid, $F = F_1$, (eq. 7) and the energy equation $R^T = 0$ is not included in the system of flow PDEs. Without loss in generality, let us assume that the jet velocities v_{jet} are applied normal to the wall. Thus, the signed jet velocities v_{jet} become $v_q^{jet} = v_{pq}^b n_{pq}^b$ (summation over p) and their sensitivity derivatives $\frac{\delta F}{\delta v_q^{jet}} = \frac{\delta F}{\delta v_{pq}^b} n_{pq}^b$. High absolute valued sensitivities pinpoint the most promising locations for the placement of jets. The sensitivity sign at these points indicates the preferred direction of the jet, i.e. suction or blowing (negative and positive sign, respectively). Such a case is illustrated in fig. 3. By solving the adjoint equations, just once, the flow control system designer makes the right decision about the optimal location of the jet.

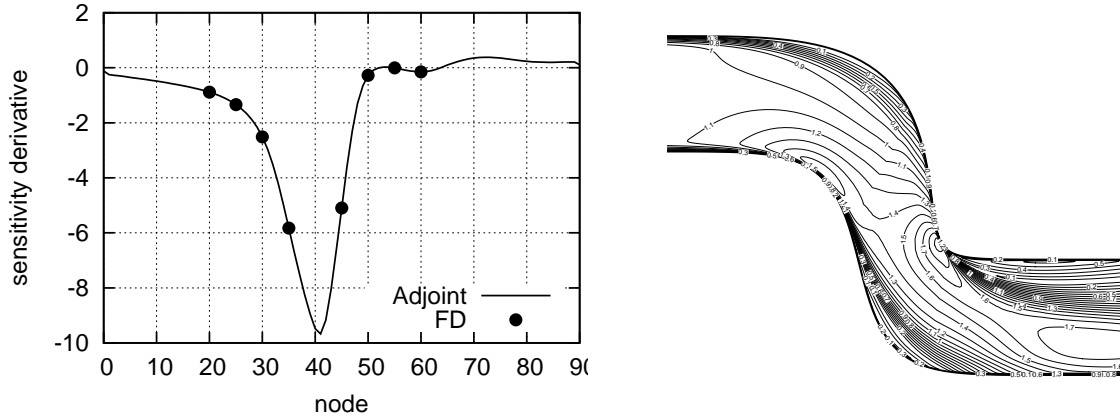


Figure 3: Flow control in an S-shaped duct for min. $F = F_1$, (eq. 7). Left: Distribution of nodal sensitivity derivatives $\frac{1}{\Delta S} \frac{\delta F}{\delta v_q^{jet}}$ along the lower wall. The sensitivities computed using the continuous adjoint method (labeled “Adjoint”) perfectly match those computed using finite differences (FD). Right: Computed velocity magnitude isolines. As a matter of fact, suction with maximum jet velocity equal to 10% of the inlet flow velocity was applied at the location recommended by just a single adjoint solution and this reduced viscous losses, expressed by F_1 (eq. 7), from 0.01835 to 0.01662.

2.4 Topology Optimization using Continuous Adjoint

In fluid mechanics, topology optimization is a useful tool for designing flow passages which connect given inlets and outlets and yield optimal performance according to the objective function F . The continuous adjoint method for the solution of topology optimization problems in incompressible flows, with or without heat transfer, was presented in [23]. Occasionally, constraints on the volume flow rates and mean temperatures per outlet boundary are imposed.

To formulate the topology optimization problem, a real-valued porosity field α is artificially introduced into the governing equations (see eqs. 2). The porosity field α that minimizes F is sought. Upon convergence of the optimization method, the local porosity values are used to identify the domain areas that correspond to the flowing fluid (nodes with $\alpha = 0$ or practically, $\alpha \leq \varepsilon$ where $\varepsilon > 0$ is an infinitesimal number). For $\alpha = 0$, eqs. 2 to 5 degenerate to the conventional flow equations. All the remaining areas with $\alpha \neq 0$ or, practically $\alpha > \varepsilon$, correspond to parts of the domain to be solidified. There, according to eqs. 2 to 5, $v_i = 0, T = T_{wall}, \tilde{v} = \nu_t = 0$. The interfaces between the two identified areas, fluid and solid, correspond to the sought optimal solid walls. The adjoint method is the perfect choice for this type of problems because the cost for computing the gradient of F is independent of the number of design variables which, in such a case, coincides with the grid size. The adjoint equations are given by eqs. 18 to 21.

The objective function considered concatenates total pressure losses (min. F_1 , eq. 7) and temperature difference (min. F_3 , eq. 9) in a single function $F = w_1 F_1 + w_3 F_3$, where w_1 and w_3 are user-defined weights.

Once the system of adjoint equations with appropriate boundary conditions has been solved, the sensitivity derivative w.r.t. α at the k -th grid node is given by the expression

$$\frac{\delta F_{aug}}{\delta \alpha_k} = (v_i u_i \Omega)_k + [(T - T_{wall}) T_a \Omega]_k + [\tilde{v} \tilde{v}_a \Omega]_k + \int_{\Omega} \tilde{v}_a \tilde{v} C_{\Delta}(\tilde{v}, \tilde{v}) \frac{\partial \Delta}{\partial \alpha_k} d\Omega \quad (27)$$

where Ω_k is the finite volume of cell k , associated with α_k . Optimal solutions to four topology optimization problems (some including flow constraints) are illustrated in fig. 4.

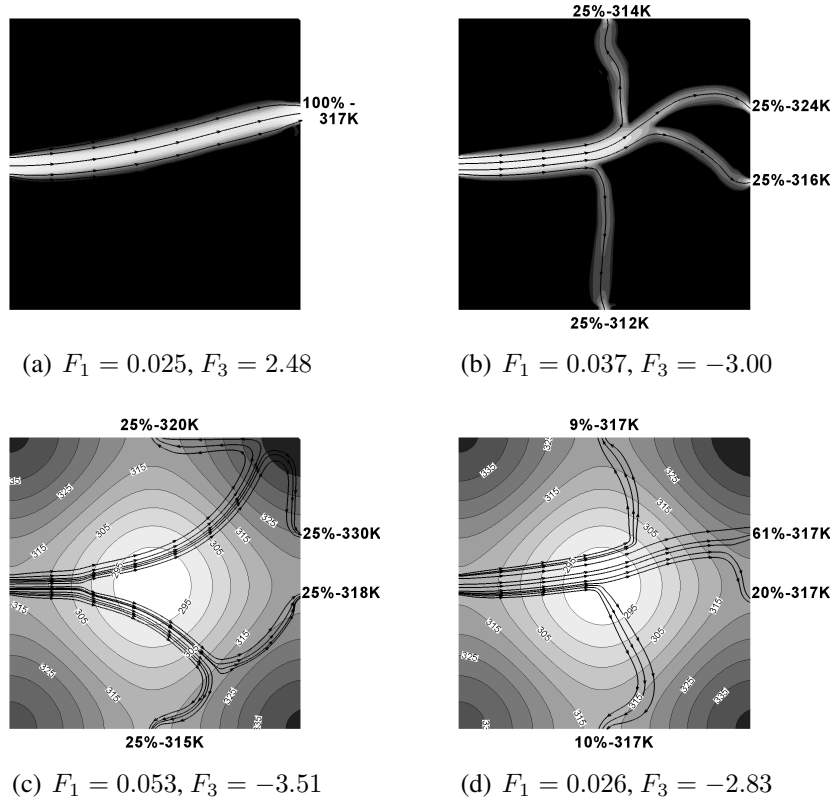


Figure 4: Unconstrained topology optimization of a one inlet/four outlet duct aiming at min. $F = F_1$ (top-left). Constrained topology optimization enforcing 25% of the incoming flow rate to exit from each outlet for, min. $F = F_1$ (top-right) and min. $F = F_1 - 0.01 F_3$ (bottom-left). Topology optimization subject to the constraint of equal mean temperature at each outlet for min. $F = F_1 + 0.01 F_3$ (bottom-right). Velocity iso-areas ((a) and (b)) or flow trajectories along with the imposed T_{wall} distribution (background in (c) and (d)).

2.5 Industrial Applications of the Continuous Adjoint Method

In fig. 5, the application of the presented adjoint approaches to three industrial problems is presented. The first case deals with the blade optimization of a 3D peripheral compressor cascade in which the objective is the minimization of entropy losses within the flow passage (min. F_4 , eq. 10), [24]. The second one is concerned with the shape optimization of a Francis turbine runner in order to achieve the desired target head H_{tar} (min. F_5 , eq. 11) and the last with the shape optimization of the Volkswagen L1 concept car, targeting minimum drag force (min. F_2 , eq. 8), [25].

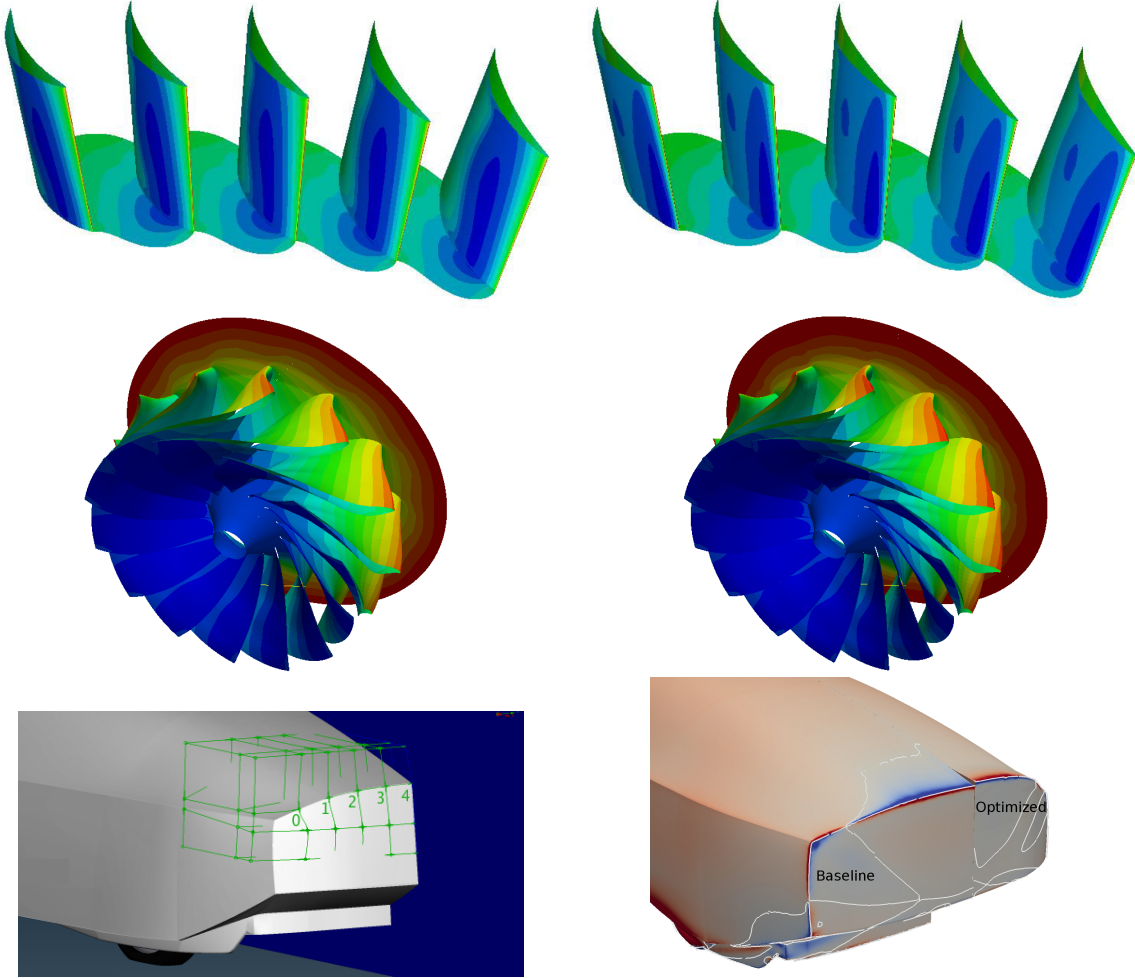


Figure 5: Top: Shape optimization of a 3D peripheral compressor cascade, targeting minimum entropy generation rate within the flow passage with constraints on the blade thickness. Pressure distributions over the initial (left) and optimal (right) blade geometries. Mid: Optimization of a Francis runner blade for increased hydraulic head (by 1.5m) subject to a number of flow constraints. Pressure distributions over the initial (left) and optimal (right) runners. Bottom: Optimization of the VW L1 concept car targeting minimum drag force. Parameterization of the rear part of the geometry by drawing morphing boxes (left) and comparative view of the baseline and optimized geometries with the corresponding sensitivity derivatives; from [25].

3 COMPUTATION OF HIGHER-ORDER SENSITIVITY DERIVATIVES

3.1 Optimization using Second-Order Sensitivity Analysis

Thus far, the optimization was based on the gradient of the objective function F w.r.t. the design variables b_m . Using this gradient, a steepest descent algorithm was used to locate the optimal solution. However, this approach usually suffers from performance degradation, as the minimum is approached in a zig-zag manner.

A remedy to this problem is to compute the Hessian matrix of F (second-order sensitivities) and apply the Newton method,

$$b_i^{k+1} = b_i^k + \delta b_i, \quad \left. \frac{\delta^2 F}{\delta b_i \delta b_j} \right|^k \delta b_j = - \left. \frac{\delta F}{\delta b_i} \right|^k \quad (28)$$

where k is the Newton iteration counter.

In aerodynamic optimization, the computation of the Hessian F subject to the constraint of satisfying the flow equations can be conducted in at least four different ways, as briefly exposed

below. All of them can be set up in either discrete or continuous form [26, 27, 28]. It is simpler, however, to present them in discrete form, where R_i and U_i stand for the discretized residual of the flow equations and the flow variables at node i , respectively. In discrete form, the first-order variation rate of F w.r.t. to $b_i, i = 1, \dots, N$ is given by

$$\frac{dF}{db_i} = \frac{\partial F}{\partial b_i} + \frac{\partial F}{\partial U_k} \frac{dU_k}{db_i} \quad (29)$$

whereas

$$\frac{dR_m}{db_i} = \frac{\partial R_m}{\partial b_i} + \frac{\partial R_m}{\partial U_k} \frac{dU_k}{db_i} = 0 \quad (30)$$

Solving eq. 30 for $\frac{dU_k}{db_i}$, at the cost of N equivalent flow solutions (EFS) and, then, computing $\frac{dF}{db_i}$ from eq. 29 is straightforward but costly and will be referred to as the Direct Differentiation (DD) method. Since its cost scales with N , the Adjoint Variable (AV) method was proposed instead. In section 2, the continuous AV method was presented. Its discrete counterpart requires the computation of the adjoint variable Ψ_i by numerically solving the adjoint system of equations

$$R_k^\Psi = \frac{\partial F}{\partial U_k} + \Psi_m \frac{\partial R_m}{\partial U_k} = 0 \quad (31)$$

and computing

$$\frac{dF}{db_i} = \frac{\partial F}{\partial b_i} + \Psi_m \frac{\partial R_m}{\partial b_i} \quad (32)$$

In discrete form, to compute the Hessian of F , the straightforward extension of the DD method for the gradient computation is the so-called DD-DD approach, in which $\frac{d^2 F}{db_i db_j}$ can be computed by

$$\frac{d^2 F}{db_i db_j} = \frac{\partial^2 F}{\partial b_i \partial b_j} + \frac{\partial^2 F}{\partial b_i \partial U_k} \frac{dU_k}{db_j} + \frac{\partial^2 F}{\partial U_k \partial b_j} \frac{dU_k}{db_i} + \frac{\partial^2 F}{\partial U_k \partial U_m} \frac{dU_k}{db_i} \frac{dU_m}{db_j} + \frac{\partial F}{\partial U_k} \frac{d^2 U_k}{db_i db_j} \quad (33)$$

where the sensitivities $\frac{d^2 U_k}{db_i db_j}$ are computed by solving ($\frac{dU_k}{db_i}$ being already known from the solution of eqs. 30).

$$\frac{d^2 R_n}{db_i db_j} = \frac{\partial^2 R_n}{\partial b_i \partial b_j} + \frac{\partial^2 R_n}{\partial b_i \partial U_k} \frac{dU_k}{db_j} + \frac{\partial^2 R_n}{\partial U_k \partial b_j} \frac{dU_k}{db_i} + \frac{\partial^2 R_n}{\partial U_k \partial U_m} \frac{dU_k}{db_i} \frac{dU_m}{db_j} + \frac{\partial R_n}{\partial U_k} \frac{d^2 U_k}{db_i db_j} = 0 \quad (34)$$

The DD-DD approach cannot avoid also the computation of $\frac{dU_k}{db_i}$ and, thus its computational cost is equal to $N + \frac{N(N+1)}{2}$ EFS in total (excluding the cost for solving the flow equations). So, the DD-DD approach scales with N^2 being too expensive for use in real-world optimization.

Two less expensive approaches to compute of the Hessian of F are the AV-DD (AV for the gradient and DD for the Hessian) and AV-AV ones. As shown in [28], both cost an many as $2N + 1$ EFS. It can be shown that, in either discrete or continuous form, the fourth alternative way, i.e. the DD-AV approach (DD for the gradient and AV for the Hessian), is the most efficient one to compute the Hessian matrix. In DD-AV, the Hessian matrix is computed by

$$\begin{aligned} \frac{d^2 F}{db_i db_j} = & \frac{\partial^2 F}{\partial b_i \partial b_j} + \Psi_n \frac{\partial^2 R_n}{\partial b_i \partial b_j} + \left(\frac{\partial^2 F}{\partial U_k \partial U_m} + \Psi_n \frac{\partial^2 R_n}{\partial U_k \partial U_m} \right) \frac{dU_k}{db_i} \frac{dU_m}{db_j} \\ & + \left(\frac{\partial^2 F}{\partial b_i \partial U_k} + \Psi_n \frac{\partial^2 R_n}{\partial b_i \partial U_k} \right) \frac{dU_k}{db_j} + \left(\frac{\partial^2 F}{\partial U_k \partial b_j} + \Psi_n \frac{\partial^2 R_n}{\partial U_k \partial b_j} \right) \frac{dU_k}{db_i} \end{aligned} \quad (35)$$

where $\frac{dU_k}{db_i}$ result from DD and Ψ_m is computed by solving the (same) adjoint equation, eq. 31. The total computational cost of DD-AV is equal to $N+1$ EFS.

The DD-AV approach for the computation of the Hessian of F can also be developed in continuous form. For instance, for an inverse design problem (min. $F = F_6$, eq. 12) in compressible aerodynamics governed by the Euler equations ($\frac{\partial f_{nk}}{\partial x_k} = 0$, where $f_{nk} = f_{nk}(U_i)$ are the inviscid fluxes and U_i the conservative flow variables), the second-order sensitivities using the DD-AV approach are given by

$$\begin{aligned}
 \frac{\delta^2 F_{aug}}{\delta b_i \delta b_j} &= \int_{S_w} \frac{\delta p}{\delta b_i} \frac{\delta p}{\delta b_j} dS + \int_{S_w} (p - p_{tar}) \frac{\delta p}{\delta b_i} \frac{\delta(dS)}{\delta b_j} + \int_{S_w} (p - p_{tar}) \frac{\delta p}{\delta b_j} \frac{\delta(dS)}{\delta b_i} \\
 &+ \frac{1}{2} \int_{S_w} (p - p_{tar})^2 \frac{\delta^2(dS)}{\delta b_i \delta b_j} + \int_{S_w} (\Psi_{k+1} p - \Psi_n f_{nk}) \frac{\delta^2 n_k}{\delta b_i \delta b_j} dS \\
 &+ \int_{S_w} \left(\Psi_{k+1} \frac{\delta p}{\delta b_i} - \Psi_n \frac{\delta f_{nk}}{\delta b_i} \right) \frac{\delta n_k}{\delta b_j} dS + \int_{S_w} \left(\Psi_{k+1} \frac{\delta p}{\delta b_j} - \Psi_n \frac{\delta f_{nk}}{\delta b_j} \right) \frac{\delta n_k}{\delta b_i} dS \\
 &+ \int_{\Omega} \frac{\partial A_{nmk}}{\partial U_l} \frac{\partial U_m}{\partial b_i} \frac{\partial U_l}{\partial b_j} \frac{\partial \Psi_n}{\partial x_k} d\Omega \\
 &- \int_{S_w} \Psi_n \left(\frac{\partial^2 f_{nk}}{\partial b_i \partial x_l} \frac{\delta x_l}{\delta b_j} + \frac{\partial^2 f_{nk}}{\partial b_j \partial x_l} \frac{\delta x_l}{\delta b_i} + \frac{\partial^2 f_{nk}}{\partial x_l \partial x_m} \frac{\delta x_l}{\delta b_i} \frac{\delta x_m}{\delta b_j} + \frac{\partial f_{nk}}{\partial x_l} \frac{\delta^2 x_l}{\delta b_i \delta b_j} \right) n_k dS \\
 &+ \int_S \Psi_n \frac{\partial}{\partial b_i} \left(\frac{\partial f_{nk}}{\partial x_k} \right) \frac{\delta x_l}{\delta b_j} n_l dS + \int_S \Psi_n \frac{\partial}{\partial b_j} \left(\frac{\partial f_{nk}}{\partial x_k} \right) \frac{\delta x_l}{\delta b_i} n_l dS \\
 &+ \int_S \Psi_n \frac{\partial f_{nk}}{\partial x_k} \frac{\delta^2 x_l}{\delta b_i \delta b_j} n_l dS + \int_S \Psi_n \frac{\partial f_{nk}}{\partial x_k} \frac{\partial}{\partial x_m} \left(\frac{\delta x_m}{\delta b_i} \right) \frac{\delta x_l}{\delta b_j} n_l dS \\
 &+ \int_S \frac{\partial \Psi_n}{\partial x_m} \frac{\partial f_{nk}}{\partial x_k} \frac{\delta x_m}{\delta b_i} \frac{\delta x_l}{\delta b_j} n_l dS - \int_S \Psi_n \frac{\partial f_{nk}}{\partial x_k} \frac{\partial}{\partial x_m} \left(\frac{\delta x_l}{\delta b_i} \right) \frac{\delta x_m}{\delta b_j} n_l dS \\
 &+ \int_S \Psi_n \frac{\partial^2 f_{nk}}{\partial x_k \partial x_l} \frac{\delta x_l}{\delta b_i} \frac{\delta x_m}{\delta b_j} n_m dS
 \end{aligned} \tag{36}$$

Here, $\frac{\delta U_k}{\delta b_i}$ and their derivatives are computed by solving the continuous DD equations

$$\frac{\delta}{\delta b_i} \left(\frac{\partial f_{nk}}{\partial x_k} \right) = \frac{\partial}{\partial b_i} \left(A_{nmk} \frac{\partial U_{mk}}{\partial x_k} \right) + \frac{\partial}{\partial x_l} \left(\frac{\partial f_{nk}}{\partial x_k} \right) \frac{\delta x_l}{\delta b_i} = 0 \tag{37}$$

where $A_{nmk} = \frac{\partial f_{nk}}{\partial U_m}$. In eq. 36, Ψ is the vector of adjoint variables computed by solving the adjoint PDEs

$$-A_{nmk} \frac{\partial \Psi_n}{\partial x_k} = 0 \tag{38}$$

Fig. 6 compares the performance of various gradient- or Hessian- based methods for the solution of the inverse design of a 2D compressor cascade. Even though the exact Newton method outperforms other methods since it requires less optimization cycles, the fact that its cost per optimization cycle scales with N makes quasi-Newton methods (such as BFGS, which approximate the Hessian matrix based on the gradient only) more efficient as N increases. In large scale ($N \gg$) industrial problems, the *exactly-initialized quasi-Newton algorithm*, in which the exact Hessian matrix is computed in the first optimization cycle only and is, then, updated using BFGS, was proposed in [28].

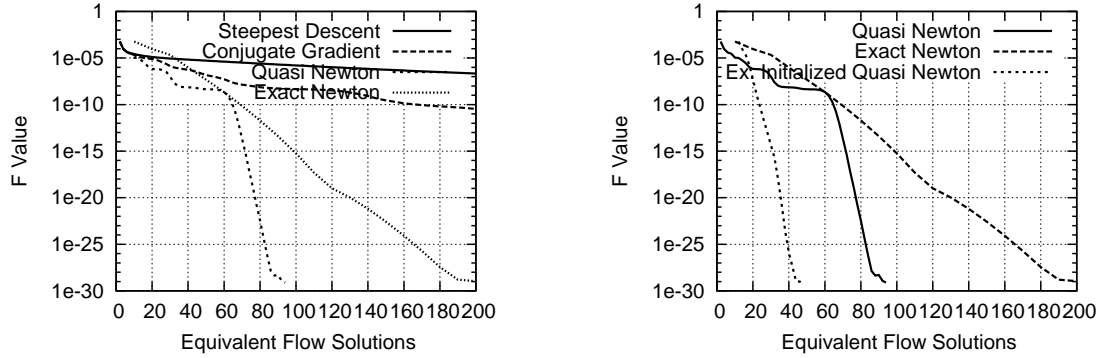


Figure 6: Inverse design of a 2D compressor cascade (min. $F = F_6$, eq. 12). Left: Reduction rate of the F value using four different optimization algorithms; steepest descent, Fletcher–Reeves conjugate gradient, BFGS quasi-Newton and exact Newton based on the DD-AV approach. Right: Reduction rate of the F value using algorithms that make use of approximate and/or exact second-order sensitivities. The first two curves correspond to standard quasi- and (exact) Newton. The third curve corresponds to the exactly-initialized quasi-Newton approach, where the exact Hessian matrix is computed in the first optimization cycle only, and then, updated using the BFGS scheme. Such a scheme is highly recommended for use in large scale optimization problems. From [28].

A much more promising way to apply Newton’s method is its truncated variant. In the truncated Newton method, [29], instead of computing the first- and second-order sensitivities of F and, then, solving eq. 28 for the corrections δb_j (N equations, $1 \leq j \leq N$), eq. 28 is solved iteratively using the *conjugate gradient* (CG) method. In this way, the computation of Hessian-vector products, instead of the Hessian matrix itself, is required. For the truncated approach, the AV-DD method is the most efficient, as proved in [29]. The truncated Newton method is ideal for large scale optimization, such as shape optimization with a lot of shape controlling variables and topology optimization, [30], which is by definition a large scale optimization problem. The efficiency of the truncated Newton method is demonstrated in fig. 7.

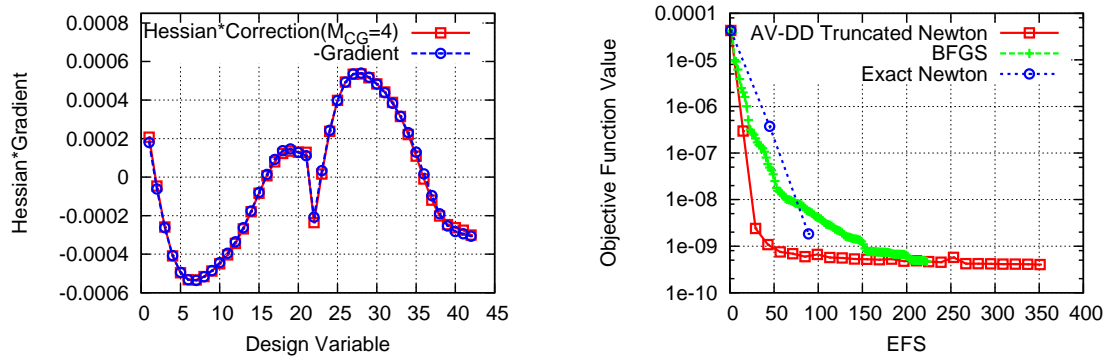


Figure 7: Design of a 2D airfoil cascade (42 degrees of freedom, min. $F = F_6$, eq. 12) using the truncated Newton method: Left: Validation of the solution of the Newton equation with $M_{CG} = 4$ conjugate gradient steps; the product of the exact Hessian matrix and the computed correction is compared to the exact gradient value. Right: Comparison of the convergence rates of the AV-DD truncated Newton method (with $M_{CG} = 4$) with other second-order methods (BFGS and exact Newton). From [29].

3.2 Solution of Robust Shape Optimization Problems

The adjoint method, coupled with DD, can also be used to solve robust design problems via a gradient-based method. In this case, higher-order derivatives must be computed as explained

below.

In aerodynamics, robust design methods aim at optimizing a shape in a range of operating conditions, or by considering the effect of environmental uncertainties, such as manufacturing imprecisions, fluctuations of the flow conditions, etc. The latter depend on the so-called environmental variables \mathbf{c} ($c_i, i \in [1, M]$). In robust design problems, the function to be minimized can be expressed as $\widehat{F} = \widehat{F}(\mathbf{b}, \mathbf{c}, \mathbf{U}(\mathbf{b}, \mathbf{c}))$, to denote the dependency of \widehat{F} on the flow variables \mathbf{U} , the design variables \mathbf{b} ($b_l, l \in [1, N]$) which parameterize the aerodynamic shape and the environmental variables \mathbf{c} ($c_i, i \in [1, M]$). Let us associate a probability density function $g(\mathbf{c})$ with \mathbf{c} . Based on $g(\mathbf{c})$, in the so-called Second-Order Second-Moment (SOSM) approach, the function \widehat{F} to be minimized in a robust design problem combines the mean value μ_F and the variance σ_F^2 of F . These are defined as

$$\mu_F(\mathbf{b}, \mathbf{c}) = \int F g(\mathbf{c}) d\mathbf{c} \simeq F + \frac{1}{2} \left[\frac{\delta^2 F}{\delta c_i^2} \right]_{\bar{\mathbf{c}}} \sigma_i^2 \quad (39)$$

$$\sigma_F^2(\mathbf{b}, \mathbf{c}) = \int (F - \mu_F)^2 g(\mathbf{c}) d\mathbf{c} \simeq \left[\frac{\delta F}{\delta c_i} \right]_{\bar{\mathbf{c}}}^2 \sigma_i^2 + \frac{1}{2} \left[\frac{\delta^2 F}{\delta c_i \delta c_j} \right]_{\bar{\mathbf{c}}}^2 \sigma_i^2 \sigma_j^2 \quad (40)$$

where the gradients are evaluated at the mean values $\bar{\mathbf{c}}$ of the environmental variables.

Based on the previous definitions, in robust design, \widehat{F} becomes

$$\widehat{F}(\mathbf{b}, \mathbf{c}) = w_1 \mu_F + w_2 \sigma_F^2 \quad (41)$$

where w_1 and w_2 are user-defined weights. It is evident that, even for computing the value of \widehat{F} , first- and second-order derivatives of F w.r.t. the environmental variables are required. Therefore, even, if the optimization problem is to be solved using a stochastic method (such as an evolutionary algorithm), the methods presented in this paper can be used to compute μ_F and σ_F^2 . If a gradient-based method is selected to solve the problem, the gradient \widehat{F} w.r.t. the design variables b_q must be available. By differentiating eq. 41 w.r.t. b_q , this becomes

$$\frac{\delta \widehat{F}}{\delta b_q} = w_1 \left(\frac{\delta F}{\delta b_q} + \frac{1}{2} \frac{\delta^3 F}{\delta c_i^2 \delta b_q} \sigma_i^2 \right) + w_2 \frac{2 \frac{\delta F}{\delta c_i} \frac{\delta^2 F}{\delta c_i \delta b_q} \sigma_i^2 + \frac{\delta^2 F}{\delta c_i \delta c_j} \frac{\delta^3 F}{\delta c_i \delta c_j \delta b_q} \sigma_i^2 \sigma_j^2}{2 \sqrt{\left[\frac{\delta F}{\delta c_i} \right]^2 \sigma_i^2 + \frac{1}{2} \left[\frac{\delta^2 F}{\delta c_i \delta c_j} \right]^2 \sigma_i^2 \sigma_j^2}} \quad (42)$$

From eq. 42, $\frac{\delta \widehat{F}}{\delta b_q}$ requires the computation of up to third-order mixed sensitivities w.r.t. c_i and b_q , such as $\frac{\delta^3 F}{\delta c_i \delta c_j \delta b_q}$. The computation of the second and third-order sensitivity derivatives is presented in detail in [31, 32]. For instance, $\frac{\delta^2 F}{\delta c_i \delta b_q}$ is computed (in continuous form) using the expression

$$\begin{aligned} \frac{\delta^2 F}{\delta c_i \delta b_q} &= \int_{S_w} (p - p_{tar}) \frac{\delta p}{\delta c_i} \frac{\delta(dS)}{\delta b_q} \\ &+ \int_{S_w} (\mathcal{L}_{k+1}^i p - \mathcal{L}_n^i f_{nk}) \frac{\delta(n_k dS)}{\delta b_q} + \int_{S_w} \left(\Psi_{k+1} \frac{\delta p}{\delta c_i} - \Psi_n \frac{\delta f_{nk}}{\delta c_i} \right) \frac{\delta(n_k dS)}{\delta b_q} \\ &- \int_{S_w} \mathcal{L}_n^i \frac{\partial f_{nk}}{\partial x_l} \frac{\delta x_l}{\delta b_q} n_k dS - \int_{S_w} \Psi_n \frac{\partial}{\partial x_l} \left(\frac{\delta f_{nk}}{\delta c_i} \right) \frac{\delta x_l}{\delta b_q} n_k dS \\ &+ \int_{S_w} \mathcal{L}_n^i \frac{\partial f_{nk}}{\partial x_k} \frac{\delta x_l}{\delta b_q} n_l dS + \int_{S_w} \Psi_n \frac{\partial}{\partial x_k} \left(\frac{\delta f_{nk}}{\delta c_i} \right) \frac{\delta x_l}{\delta b_q} n_l dS \end{aligned} \quad (43)$$

where the $\mathcal{L}_n^i = \frac{\delta \Psi_n}{\delta c_i}$ fields ($i = 1, M$) are computed by solving the following system of PDEs

$$-A_{nmk} \frac{\partial \mathcal{L}_n^i}{\partial x_k} - \frac{\delta A_{nmk}}{\delta c_i} \frac{\partial \Psi_n}{\partial x_k} = 0 \quad (44)$$

derived from the DD of the adjoint equations w.r.t. the environmental variables. The third-order mixed sensitivity derivatives of F , required by eq. 42, are obtained from the differentiation of eq. 43 which is omitted in the interest of space.

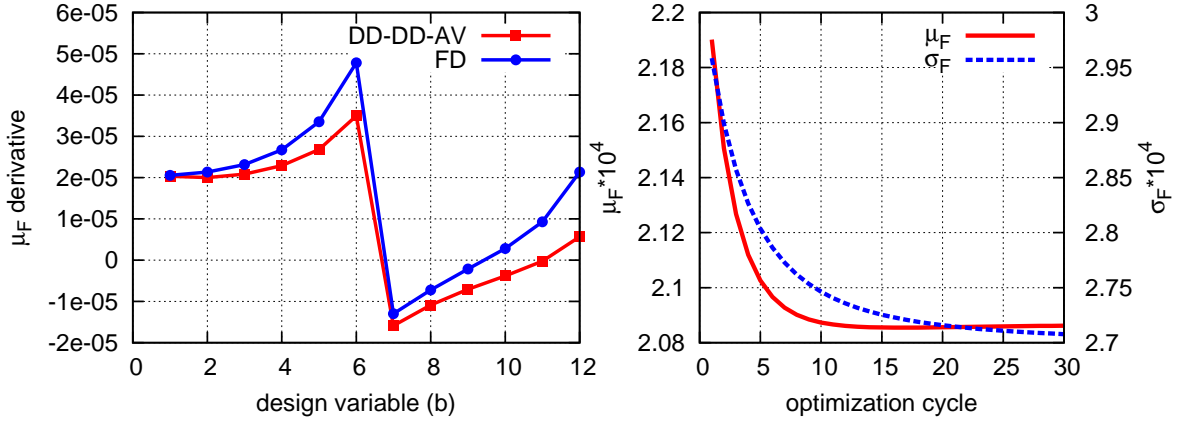


Figure 8: Robust inverse design of a 2D symmetric cascade (min. $F = F_6$, eq. 12). Left: Comparison of sensitivities $\frac{\delta \mu_F}{\delta b_q}$ (b_q are the coordinates of Bézier control points) computed using the proposed method and finite differences (FD). Right: convergence of the mean value and standard deviation of F using $w_1 = 0.7, w_2 = 0.3$. From [32].

Acknowledgments

Parts of the relevant research were funded by Volkswagen AG (Group Research, K-EFFG/V, Wolfsburg, Germany) and Icon Technology and Process Consulting Ltd. Research related to topology optimization and the computation of second-order derivatives was partially supported by Basic Research projects funded by the National Technical University of Athens.

REFERENCES

- [1] I.C. Karpolis, X.S. Trompoukis, V.G. Asouti, K.C. Giannakoglou: CFD-based analysis and two-level aerodynamic optimization on Graphics Processing Units: *Computer Methods in Applied Mechanics and Engineering*, 199 (2010), 712-722.
- [2] V.G. Asouti, X.S. Trompoukis, I.C. Karpolis, K.C. Giannakoglou: Unsteady CFD computations using vertex-centered finite volumes for unstructured grids on Graphics Processing Units. *International Journal for Numerical Methods in Fluids*, 67 (2011), 232-246.
- [3] A.S. Zymaris, D.I. Papadimitriou, K.C. Giannakoglou, C. Othmer: Continuous adjoint approach to the Spalart-Allmaras turbulence model for incompressible flows, *Computers & Fluids*, 38 (2009), 1528-1538.
- [4] A.S. Zymaris, D.I. Papadimitriou, K.C. Giannakoglou, C. Othmer: Adjoint wall functions: A new concept for use in aerodynamic shape optimization, *Journal of Computational Physics*, 229 (2010), 5228-5245.

- [5] O. Pironneau: On optimum design in fluid mechanics. *Journal of Fluid Mechanics*, 64 (1974), 97-110.
- [6] A. Jameson: Aerodynamic design via control theory. *Journal of Scientific Computing*, 3 (1988), 233-260.
- [7] W.K. Anderson, V. Venkatakrishnan: Aerodynamic design optimization on unstructured grids with a continuous adjoint formulation. *AIAA Paper*, 97-0643, 1997.
- [8] E. Arian, M.D. Salas: Admitting the inadmissible: Adjoint formulation for incomplete cost functionals in aerodynamic optimization. NASA/CR-97-206269, ICASE Report No.97-69, 1997.
- [9] S. Hazra, V. Schulz, J. Brezillon, N. Gauger: Aerodynamic shape optimization using simultaneous pseudo-timestepping. *Journal of Computational Physics*, 204 (2005), 46-64.
- [10] D.I. Papadimitriou, K.C. Giannakoglou: A continuous adjoint method with objective function derivatives based on boundary integrals for inviscid and viscous flows. *Journal of Computers and Fluids*, 36 (2007), 325-341.
- [11] C. Othmer: A continuous adjoint formulation for the computation of topological and surface sensitivities of ducted flows. *International Journal for Numerical Methods in Fluids*, 58 (2008), 861-877.
- [12] G.R. Shubin, P.D. Frank: A comparison of the implicit gradient approach and the variational approach to aerodynamic design optimization. Boeing Computer Services Report AMS-TR-163, 1991.
- [13] G.W. Burgreen, O. Baysal: Three-dimensional aerodynamic shape optimization using discrete sensitivity analysis. *AIAA Journal*, 34 (1996), 1761-1770.
- [14] J. Elliot, J. Peraire: Aerodynamic design using unstructured meshes. *AIAA Paper* 96-1941, 1996.
- [15] M.C. Duta, M.B. Giles, M.S. Campobasso: The harmonic adjoint approach to unsteady turbomachinery design. *International Journal for Numerical Methods in Fluids*, 40 (2002), 323-332.
- [16] C.S. Kim, C. Kim, O.H. Rho: Feasibility study of constant eddy-viscosity assumption in gradient-based design optimization. *Journal of Aircraft*, 40(2003), 1168-1176.
- [17] B.J. Lee, C. Kim: Automated design methodology of turbulent internal flow using discrete adjoint formulation. *Aerospace Science and Technology*, 11 (2007), 163-173.
- [18] D.J. Mavriplis: Discrete adjoint-based approach for optimization problems on three-dimensional unstructured meshes. *AIAA Journal*, 45 (2007), 740-750.
- [19] A. Bueno-Orovio, C. Castro, F. Palacios, E. Zuazua: Continuous Adjoint Approach for the SpalartAllmaras Model in Aerodynamic Optimization *AIAA Journal*, 50 (2012), 631-646.
- [20] W. Jones, B. Launder: The prediction of laminarization with a two-equation model of turbulence. *International Journal of Heat And Mass Transfer*, 15 (1972), 301-314.

- [21] E. Stanewsky: Adaptive wing and flow control technology. *Progress in Aerospace Sciences*, 37 (2001), 583–667.
- [22] A.L. Braslow: A history of suction-type laminar flow control with emphasis on flight research. *NASA Monographs*, vol. 13, 1999.
- [23] E.M. Papoutsis-Kiachagias, E.A. Kontoleontos, A.S. Zymaris, D.I. Papadimitriou, K.C. Giannakoglou: Constrained topology optimization for laminar and turbulent flows, including heat transfer. *EUROGEN Conference 2011*, Capua, Italy.
- [24] D.I. Papadimitriou, K.C. Giannakoglou: Compressor blade optimization using a continuous adjoint formulation. *ASME TURBO EXPO*, GT2006/90466, 8-11 May 2006, Barcelona, Spain.
- [25] C. Othmer, E. Papoutsis-Kiachagias, K. Haliskos: CFD Optimization via Sensitivity-Based Shape Morphing. *4th ANSA & μ ETA International Conference*, Thessaloniki, Greece, 2011.
- [26] D.I. Papadimitriou, K.C. Giannakoglou: Computation of the Hessian matrix in aerodynamic inverse design using continuous adjoint formulations. *Computers & Fluids*, 37 (2008), 1029–1039.
- [27] D.I. Papadimitriou, K.C. Giannakoglou: The continuous direct-adjoint approach for second-order sensitivities in viscous aerodynamic inverse design problems, *Computers & Fluids*, 38 (2008), 1539–1548.
- [28] D.I. Papadimitriou, K.C. Giannakoglou: Aerodynamic shape optimization using adjoint and direct approaches, *Archives of Computational Methods in Engineering*, 15 (2008), 447–488.
- [29] D.I. Papadimitriou, K.C. Giannakoglou: Aerodynamic Design using the Truncated Newton Algorithm and the Continuous Adjoint Approach. *International Journal for Numerical Methods in Fluids*, 68 (2012), 724-739.
- [30] D.I. Papadimitriou, E.M. Papoutsis Kiachagias, K.C. Giannakoglou: Topology Optimization in Fluid Dynamics Using Adjoint-Based Truncated Newton. *European Congress on Computational Methods in Applied Sciences and Engineering (ECCOMAS 2012)*, Vienna, Austria, September 10-14, 2012.
- [31] E.M. Papoutsis-Kiachagias, D.I. Papadimitriou, K.C. Giannakoglou: Robust design in aerodynamics using third-order sensitivity analysis based on discrete adjoint. Application to quasi-1D flows. *International Journal for Numerical Methods in Fluids*, 69 (2012), 691-709.
- [32] E.M. Papoutsis-Kiachagias, D.I. Papadimitriou, K.C. Giannakoglou: On the optimal use of adjoint methods in aerodynamic robust design problems. *CFD and OPTIMIZATION 2011, ECCOMAS Thematic Conference*, Antalya, Turkey, 2011.